buildings

MDPI

Article

Experimental Study on Axial Compression of Bamboo Scrimber Cold-Formed Thin-Walled Steel Composite Special-Shaped Columns

Chao Lei [1], Yuhao Wu [1], Bingyang Yang [1], Bingbing Wang [1], Jianqiang Han [1,2,*] and Xiuyan Fu [1]

[1] College of Civil and Architectural Engineering, North China University of Science and Technology, Tangshan 063210, China; 15116323777@163.com (C.L.); wu2393461360@163.com (Y.W.); fuxiyan@ncst.edu.cn (X.F.)
[2] Key Laboratory of Earthquake Engineering and Disaster Prevention of Hebei Province, Tangshan 063210, China
* Correspondence: hjq@ncst.edu.cn; Tel.: +86-15032587758

Abstract: As one of the four key sectors for energy saving and emissions reduction, the construction industry faces ongoing high energy consumption and emissions. To support China's sustainable development, urgent promotion of green construction and energy-saving measures is necessary. This led to the proposal of nine specimens of L-shaped, T-shaped, and cross-shaped engineered bamboo, cold-formed thin-walled steel, and their combinations for axial compression tests to study the effect of bamboo–steel structures on axial compression performance. The results showed that the load-bearing capacity of the three bamboo–steel composite columns increased by 19.5–21.4% compared to the sum of steel composite and L-shaped bamboo composite columns, significantly enhancing overall stability and deformation capacity. The synergy between steel and engineered bamboo effectively addressed the instability issues of steel structures with large width-to-thickness ratios. Using Abaqus finite element software for simulation, the stress distribution at failure and load-displacement curves were closely aligned with experimental outcomes. The study presents a formula for calculating the axial compression capacity of cold-formed thin-walled steel-engineered bamboo composite columns, with theoretical and experimental discrepancies within 13.28%, offering a theoretical basis for the design of engineered bamboo–steel composite columns.

Keywords: cold-formed thin-walled steel; reorganized bamboo; special-shaped column; axial compression

Citation: Lei, C.; Wu, Y.; Yang, B.; Wang, B.; Han, J.; Fu, X. Experimental Study on Axial Compression of Bamboo Scrimber Cold-Formed Thin-Walled Steel Composite Special-Shaped Columns. *Buildings* **2024**, *14*, 3959. https://doi.org/10.3390/buildings14123959

Academic Editor: Mizan Ahmed

Received: 19 November 2024
Revised: 7 December 2024
Accepted: 9 December 2024
Published: 13 December 2024

1. Introduction

In recent years, with the rapid development of China's economy, the scale of the construction industry has been expanded and the technical strength has been obviously improved. As one of the four key sectors for energy-saving and emissions reduction, the construction industry faces ongoing high energy consumption and emissions [1]. To support the objectives of China's sustainable development, urgent promotion of green construction and energy-saving measures is necessary. With vast resources and a large population, China has been engaged in housing construction since ancient times. In recent years, with the continuous updating of China's smelting process and the continuous increase of steel production, China has become a steel power. With the unique advantages of raw materials, steel structure has a wider range of applications. The cold-formed thin-walled steel structure system has been applied in many forms in China. With the advantages of light structural mass, good anti-seismic performance, flexible and diversified cross-section forms, easy processing, and environment-friendly and recyclable building materials, etc., it has wide applicability [2]. In recent years, logging has been strictly prohibited in China, and there is a large demand for timber. Meanwhile, bamboo, as an original product in China, has numerous types, strong adaptability, wide distribution, and many advantages. Raw bamboo is convenient to obtain, low in price, and short in maturity duration, and it is an excellent raw material for construction [3–7].

With the constant improvement of specifications for cold-formed thin-walled steel and bamboo scrimber, the study of cold-formed thin-walled steel has developed from the ground floor to high-rise buildings, and domestic and foreign scholars are devoted to studying the physical properties of bamboo scrimber and cold-formed thin-walled steel composite structures [8,9]. In the study of the built-in reinforced bamboo scrimber column, it is found that the ultimate bearing capacity, rigidity, and ductility of the specimen can be improved by increasing the reinforcement ratio of the specimen. When the stirrup ratio is not changed, the increase in slenderness ratio will lead to a decrease in rigidity, ductility, and ultimate bearing capacity of the specimen, further causing the failure state to change from adhesive layer failure to buckling failure [10]. The bearing capacity of the steel–bamboo composite structure is in proportion to the slenderness ratio of the specimen and the width–thickness ratio of the section. The two materials have an obvious combination effect, and the specimen shows good bearing capacity and ductility, which indicates that the two materials collaborate well [11–13]. The bamboo scrimber improves the problem of easy instability for the cold-formed thin-walled steel section due to the large width–thickness ratio, and the cold-formed thin-walled steel also inhibits the deformation and failure of the bamboo scrimber [14–18]. In the case of loading the same load, the weight of reconstituted bamboo is lighter than that of other woods, reducing the self-weight of the building and having unique advantages as a load-bearing component [19,20].

Combined with relevant research in China and abroad, this paper proposes bamboo scrimber cold-formed thin-walled steel composite special-shaped column specimens of L-shape, T-shape, and cross-shape. All the contact surfaces of L-shaped cold-formed thin-walled steel and bamboo scrimber are bonded with epoxy resin adhesive, and the bonded specimen is reinforced with bolts to ensure the integrity of the composite special-shaped column. The specific form of the composite column is shown in Figure 1. Through the axial compression test, the axial compression bearing capacity of each special-shaped column is obtained. In the paper, the failure mechanism of the bamboo–steel composite special-shaped column is obtained by exploring the experimental phenomena and the failure status as well as analyzing the experimental data, and a reasonable formula for calculating the axial compression bearing capacity is put forward by comparing the improvement in the overall stability and deformation capacity of the specimen from the bamboo–steel composite special-shaped column. The structure of the steel–bamboo composite special-shaped column combines the advantages of the integral aesthetic sense, the flexible function design, and the excellent bearing performance of the building so that the construction industry in China will enter a brand-new period of progress in the future, and the composite structure will inevitably have a wider application range and better development.

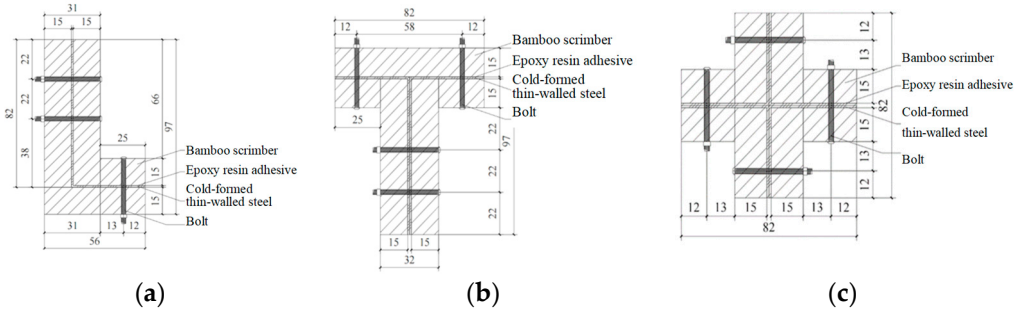

Figure 1. The specific size of the composite column. (**a**) Section of L-shaped bamboo–steel composite special-shaped column; (**b**) Section of T-shaped bamboo–steel composite special-shaped column; (**c**) Section of cross-shaped bamboo–steel composite special-shaped column.

2. Experiment Overview

2.1. Design of Experiment

In the experiment, nine composite special-shaped columns of L-shaped, T-shaped, and cross-shaped bamboo scrimber composite special-shaped columns, cold-formed thin-

walled steel composite special-shaped columns, and bamboo scrimber cold-formed thin-walled steel composite special-shaped columns are designed, as shown in Table 1. The thickness of the steel is 1 mm, and the length of the specimen is 1200 mm. Place the polished steel profile and the reorganized bamboo board on a horizontal surface and place the side to be coated with glue on it. Mix the epoxy resin glue HB-826 according to the ratio of 1:1; within 10 min, the epoxy resin glue evenly coats in the reorganization of the bamboo board and the steel section, and the thickness of the glue coating is about 1 mm. Then, with the reorganization of the bamboo board and steel according to the design of the splicing, the use of fixtures will be fixed so that the steel and reorganization of bamboo between the epoxy resin adhesive is evenly distributed and will overflow, the excess epoxy resin adhesive wiped away, placed for 24 h. After the completion of the combination of the components, the electric drill will be used to drill the bolts into design position (bolt size of M5 mm × 50 mm, the vertical spacing is 200 mm). When the bolts are just, all in the member of the internal stop so that each bolt is into the member of the same depth, this will ensure the integrity of the combination of components during the test. For the specific dimensions, see Table 1.

Table 1. Design parameters of bamboo–steel composite special-shaped columns.

Specification	No.	Specimen Size/(mm)	Slenderness Ratio
L-shaped column	L-G-Z	82 × 41 × 1	71.8
	L-Z-Z	96 × 55 × 30 × 30	62.1
	L-G-Z-Z	97 × 56 × 31 × 31	38.4
T-shaped column	T-G-Z	82 × 82 × 2 × 1	61.3
	T-Z-Z	80 × 66 × 30 × 30	46.7
	T-G-Z-Z	82 × 66 × 31 × 32	45.4
Cross-shaped column	S-G-Z	82 × 82 × 2 × 2	50.0
	S-Z-Z	80 × 80 × 30 × 30	44.4
	S-G-Z-Z	82 × 82 × 32 × 32	43.1

2.2. Material Property Test

The bamboo scrimber plate in the composite column adopts phyllostachys pubescens as the raw material, and the cold-formed thin-walled steel adopts the model of Q235. The mechanical properties are measured again for the materials in the uniform batch used in the text.

2.2.1. Compressive Strength Test of Bamboo Scrimber Along the Grain

The compression specimens of bamboo scrimber along the grain in this test are designed according to the "Standard for Methods Testing of Timber Structures" (GB/T50329-2012) [21] and "Bamboo Scrimber" (GB/T40247-2021) [22]. The specimens have the dimensions of 15 mm × 25 mm × 105 mm, with the reference number KY1~KY6, and there are six specimens in total. The section size of the specimen is shown in Figure 2. The WAW-300 electro-hydraulic servo universal testing machine is used for carrying out the loading test, and displacement loading is adopted. The initial load is 5% of the failure load, and the specimen is uniformly loaded at the loading speed of 4.5 mm/min; the loading time is stipulated in 30–90 s. Before loading, the specimen was placed in a constant temperature environment and dried, the force sensor was placed vertically at the bottom of the testing machine, and the specimen was placed on the sensor. The axial line of the specimen coincided with the center of the reaction frame, and the displacement was loaded at a uniform speed until the specimen was damaged.

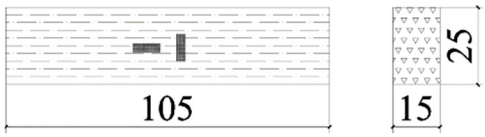

Figure 2. Compression specimens along the grain.

For the compression specimen of bamboo scrimber along the grain, there are mainly two failure modes of creasing failure and "Y"-shaped failure. The failures of the compression specimens are shown in Figure 3. In the elastic stage, the stress increases uniformly with the strain, and it presents a linear increase integrally; when entering the elastic-plastic stage, the stress increases slowly with the strain, with a gentler slope for the curve; and in the plastic stage, the slope remains basically unchanged, the strain changes quickly, and finally the specimen fails. The stress–strain curve of the compression specimen is as shown in Figure 4.

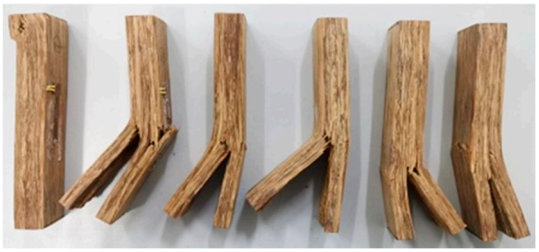

Figure 3. Failure state of bamboo scrimber compressive specimen.

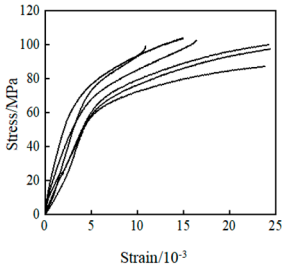

Figure 4. Stress–strain curve of bamboo scrimber compressive specimen.

Calculate the elastic modulus and compressive strength for the compression specimen of bamboo scrimber along the grain according to the specification of "Bamboo Scrimber", and calculate the compressive elastic modulus Ec according to Formula (1):

$$E_c = \frac{\Delta P}{bh\Delta\varepsilon} \tag{1}$$

wherein ΔP is the load difference at the linear stage, $\Delta\varepsilon$ is the strain difference corresponding to the load difference, b is the width of the specimen, and h is the thickness of the specimen.

The compressive strength is calculated according to Formula (2):

$$\sigma_c = \frac{P_{max}}{bh} \tag{2}$$

wherein P_{max} is the maximum value for compression failure of the specimen, b is the width of the specimen, and h is the thickness of the specimen.

The average value for compressive strength of the bamboo scrimber along the grain is 98.49 MPa, and the average value for elastic modulus is 15,006.01 MPa. According to the requirements in the specification of "Bamboo Scrimber", the bamboos in this batch are high-class products with a compressive strength of grade 120Ec. Table 2 shows the compression test results of the bamboo scrimber along the grain.

Table 2. Results of compression test of bamboo scrimber along the grain.

No.	Ultimate Load/kN	Compressive Strength/MPa	Compressive Elastic Modulus/MPa
KY1	36.61	97.63	14,620.33
KY2	32.75	87.33	11,149.61
KY3	39.01	104.03	21,667.00
KY4	37.52	100.05	8960.23
KY5	37.23	99.28	18,289.34
KY6	38.49	102.64	15,349.53
Average value	36.94	98.49	15,006.01
Standard deviation	2.23	5.94	4219.78
Coefficient of variation	6.04%	6.03%	28.12%

2.2.2. Tensile Strength Test of Bamboo Scrimber Along the Grain

The tensile specimens of bamboo scrimber along the grain in this test are designed according to "Bamboo Scrimber" (GB/T40247-2021) [22] and the "Method of Testing in Tensile Strength Parallel to Grain of Wood" (GB/T1938-2009) [23]. The specimens have the dimensions of 15 mm × 7 mm. Six tensile specimens of bamboo scrimber along the grain are processed in total, with the reference number KL1~KL6, and the size of the specimen is shown in Figure 5. The WAW-300 electro-hydraulic servo universal testing machine is used for carrying out the loading test, and displacement loading is adopted. The specimen is constantly loaded at the loading speed of 3 mm/min. The loading time is stipulated to be from 30 to 90 s. Before loading, Caffert glue is applied to the strain gauge on the specimen for protection. After the specimen is placed and dried in a constant temperature environment, it is vertically fixed in the middle of the chuck of the testing machine. The axial line of the specimen coincides with the center of the upper and lower chuck, and then the test is completed.

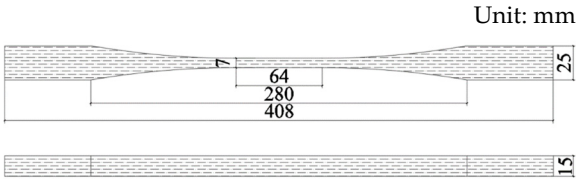

Figure 5. Tensile specimens along the grain.

For the tensile specimens of bamboo scrimber along the grain, there are mainly three failure modes of diagonal-crack failure, V-shaped failure, and Z-shaped failure. The failures of the tensile specimens are shown in Figure 6. The test of the tensile specimen is divided into two stages. In the linear stage, the curve slope is constant, and the strain increases uniformly with the increase of stress; when the specimen reaches the maximum load, the specimen rapidly fails, and the load drops rapidly. The stress–strain curve of the tensile specimen is shown in Figure 7.

Figure 6. Failure state of bamboo scrimber tensile specimen.

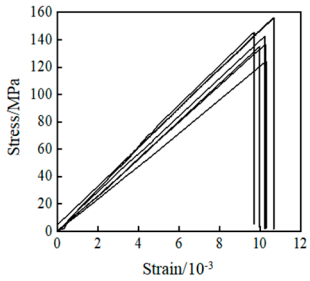

Figure 7. Stress-strain curve of recombinant bamboo tensile specimen.

The elastic modulus and the tensile strength for the tensile specimen of bamboo scrimber along the grain are calculated according to the specification of "Bamboo Scrimber", and the tensile elastic modulus is calculated according to the Formula (3):

$$E_t = \frac{\Delta P}{bh\Delta\varepsilon} \tag{3}$$

wherein ΔP is the load difference at the linear stage, $\Delta\varepsilon$ is the strain difference corresponding to the load difference, b is the width of the specimen, and h is the thickness of the specimen.

The tensile strength is calculated according to Formula (4):

$$\sigma_t = \frac{P_{max}}{bh} \tag{4}$$

wherein $Pmax$ is the maximum value for tensile failure of the specimen, b is the width of the specimen, and h is the thickness of the specimen.

The average value for tensile strength of the bamboo scrimber along the grain is 139.99 MPa, and the average value for elastic modulus is 13,877.80 MPa. According to the requirements in the specification of "Bamboo Scrimber", the bamboos in this batch are high-class products with a tensile strength of grade 120Et. Table 3 shows the tensile test results of the bamboo scrimber along the grain.

Table 3. The results of the tensile test of bamboo scrimber along the grain.

No.	Ultimate Load/kN	Tensile Strength/MPa	Tensile Elastic Modulus/MPa
KL1	14.33	136.48	13,353.97
KL2	16.37	155.90	14,343.47
KL3	14.19	135.14	13,170.17
KL4	15.28	145.53	16,958.27
KL5	14.98	142.67	13,430.44
KL6	13.04	124.19	12,010.69
Average value	14.70	139.99	13,877.80
Standard deviation	1.03	9.80	1536.64
Coefficient of variation	7.00%	7.00%	11.07%

2.2.3. Tensile Strength Test of Cold-Formed Thin-Walled Steel

The specimens used in the test are designed and processed according to the "Technical Code of Cold-formed Thin-Wall Steel Structures" (GB 50018-2002) [24], and three groups of tensile specimens are made, with a thickness of 1.0 mm. The tensile specimen is shown in Figure 8. The WDW-100 electro-hydraulic servo universal testing machine is used to complete the tensile test. The specimens, numbered G1, G2, and G3, are constantly loaded with force at the loading rate of 120 N/s until failed, and the loading time is ensured to be about 60 s. The failure state of the specimens is shown in Figure 9.

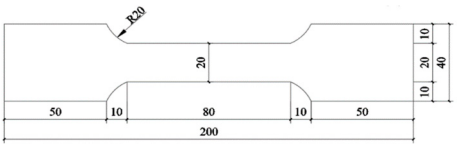

Figure 8. Steel tensile specimens.

Figure 9. Failure state of steel tensile specimens.

Before loading the epoxy resin adhesive coated in the specimen on the strain gauge for protection, the specimen will be placed in a constant temperature environment after drying to maintain the vertical fixed in the middle of the test machine chuck; the specimen rolling direction axis and the upper and lower center of the chuck coincide with the distance between the chuck for the specimen of the original distance, the use of force loading until the destruction of the specimen, the record of the destruction of loads.

At the initial stage of loading, there is no obvious change in the specimen. With the increase of the load, the obvious necking phenomenon can be observed in the middle area of the specimen, and finally, a crisp sound is heard, and the specimen fails. For the cold-formed thin-walled steel tensile specimens, all failures are located in the middle of the specimens where the strain gauges are pasted. Table 4 shows the tensile test results of cold-formed thin-walled steel.

Table 4. Steel tensile test results.

No.	Ultimate Load/kN	Tensile Strength/MPa	Tensile Elastic Modulus/MPa
G1	6.49	324.59	169,747.23
G2	7.45	372.25	183,378.95
G3	7.31	365.33	137,287.24
Average value	7.08	354.06	163,471.14
Standard deviation	0.42	21.03	19,333.10
Coefficient of variation	5.98%	5.94%	11.83%

2.3. Test Scheme and Arrangement of Measuring Points

The specimen is subjected to the axial compression test on a 200 t electro-hydraulic servo pressure testing machine. The length of the specimen is 1200 mm. The upper bearing plate of the testing machine is a hinged support, and the lower bottom plate is provided with a self-made hinged support. The test adopts displacement control, and the loading rate is 0.005 mm/s. When loading to the ultimate load, continue to load, and stop when the load drops to 50% of the ultimate load. In order to better measure the stress–strain of the specimen, the test will be arranged in the strain gauge at the column height of 1/2 in the external reorganization of the bamboo, and the internal cold-formed thin-walled steel sections will be pasted on the same position of the strain gauge; at the same time, in the external reorganization of the bamboo strain gauge on the same height of the arrangement of the displacement meter, to prevent contact with the strain gauge resulting in inaccurate measurement data, will be placed in the displacement meter pointer on the side of the

strain gauge. Displacement and strain are collected with the Gantner data acquisition instrument. The layout of the cross-shaped strain gauges and the displacement gauges are as shown in Figure 10.

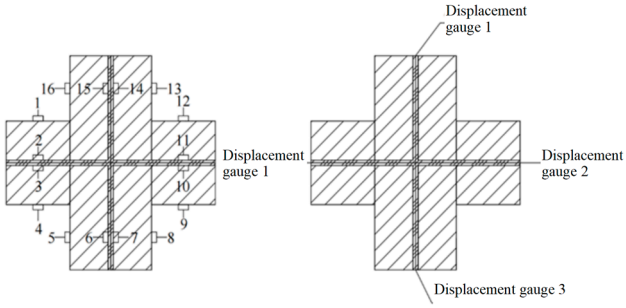

Figure 10. Layout of strain gauges and displacement meters for cross-shaped steel–bamboo composite columns.

In the preparation stage, the strain gauges and displacement gauges pasted on the specimen were connected to the collector one by one, and the strain gauges and displacement gauges were checked on the test computer to see if they were normal. In this test, the force transducer is placed in the center of the lower base plate of the testing machine, the homemade hinge support is placed in the center above the force transducer, and a layer of fine sand is laid on the upper surface of the hinge support to ensure that the specimen is subjected to a uniform force during the test.

During the test phase, the combined column is placed in the middle position of the hinge support, the distance between the top plate of the hydraulic press and the specimen is adjusted to about 10 mm, the combined column is physically aligned, and the top plate of the hydraulic press is adjusted to contact with the combined column at the end of the alignment.

Set the preload to about 10% of the estimated ultimate load, check whether the displacement gauge and strain gauges work well, and adjust the position of the combined column by observing the numerical size of all the strain gauges to ensure that the combined column is axially pressurized. The test adopts displacement control, with a loading rate of 0.005 mm/s, loading to the ultimate load in order to get the falling section of the load-displacement curve; continue to load until the load falls to 85% of the ultimate load. When loading stops, the test is over.

3. Test Results and Analysis

3.1. Test Phenomenon

The specimen L-G-Z is an L-shaped steel column. During the loading process, the specimen has obvious distortional buckling of the wave shape. When the specimen is loaded to about 5 kN, the middle part of the flange is bent. The ultimate bearing capacity of the final specimen is 5.7 kN, at which the bending and buckling failure occurs. The failure of the specimen is shown in Figure 11.

The specimen L-Z-Z is an L-shaped bamboo scrimber column. When it is loaded to about 79 kN, the specimen is observed to start bending, and a slight sound of adhesive cracking is heard. When the specimen is continuously loaded to 81 kN, it reaches the ultimate bearing capacity, obvious bending occurs, and the bending instability failure finally occurs. The failure of the specimen is shown in Figure 12.

The specimen L-G-Z-Z is an L-shaped steel–bamboo scrimber column. When the load reaches about 40 kN, the steel inside the specimen is subjected to wave buckling, with a slight sound of adhesive cracking occasionally. When the specimen is continuously loaded to 61 kN, the buckling amplitude of the steel inside the specimen increases, the frequency of the adhesive cracking sound increases, and the specimen is observed to start bending integrally. When the load reaches about 105 kN, the specimen reaches the ultimate bearing

capacity, and bending instability and glue failure finally occur. The failure of the specimen is shown in Figure 13.

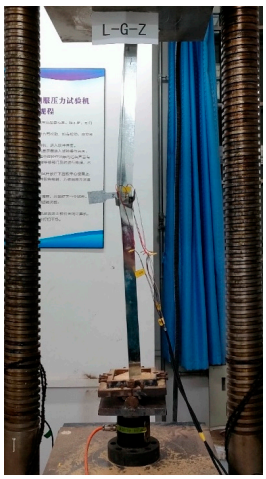

Figure 11. L-G-Z destroying figure.

Figure 12. L-Z-Z destroying figure.

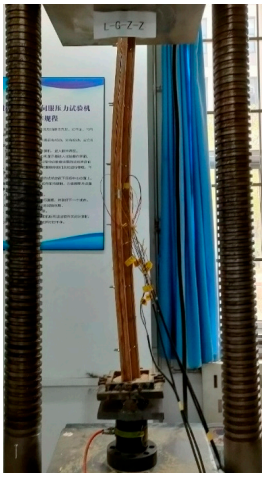

Figure 13. L-G-Z-Z destroying figure.

The specimen T-G-Z is a T-shaped steel column. When the specimen is loaded to about 4.6 kN, the flange on one side of the specimen begins to bend, and a gap appears at the

middle-lower end of the two L-shaped steels. When the specimen is continuously loaded to about 8 kN, the flange on the other side of the specimen begins to bend, and the web bends towards the flange direction. When the load reaches about 14 kN, the specimen reaches the ultimate bearing capacity, and distortional buckling occurs in the middle part on one side of the flange. The final failure mode of the specimen involves distortional buckling and flexural-torsional buckling, and the failure of the specimen is shown in Figure 14.

Figure 14. T-G-Z destroying figure.

The specimen T-Z-Z is a T-shaped bamboo scrimber column, and there is no phenomenon in the early loading stage. When the specimen is loaded to about 139 kN, the specimen makes a slight sound of glue failure and begins to bend integrally. When the specimen is continuously loaded to about 171 kN, the specimen reaches the ultimate bearing capacity, the overall bending effect is obvious, and the specimen is subjected to overall bending failure. The failure of the specimen is shown in Figure 15.

Figure 15. T-Z-Z destroying figure.

The specimen T-G-Z-Z is a T-shaped steel–bamboo scrimber column. When the specimen is loaded to about 73 kN, the steel in the middle of the web begins to buckle, and the specimen is slightly bent. When it is continuously loaded to about 105 kN, the steel in the middle of the flange on one side of the specimen begins to buckle, and the force basically increases linearly. When the specimen is loaded to about 190 kN, load fluctuation occurs, and consequently, the load-bearing capacity continues to increase. It is observed that the gap between the flange steels is relatively large, and the buckling is serious. The specimen has obvious buckling integrally. When the load reaches about 221 kN, the specimen reaches

the ultimate bearing capacity, and the ultimate failure of the specimen is instability failure, glue failure, and plate-buckling failure. The failure of the specimen is shown in Figure 16.

Figure 16. T-G-Z-Z destroying figure.

The specimen S-G-Z is a cross-shaped steel column. When the load reaches about 6 kN, a gap begins to appear between the rear flange and the upper part of the right flange, and weak buckling occurs in the local part. When the load reaches about 15 kN, the axial displacement increases, the gap between the two flanges continuously increases, and the distortional buckling is obvious. The wave-type buckling phenomenon occurs in the front flange, and the sound is given out continuously under continued loading. When the load reaches about 22 kN, the specimen is twisted integrally, the bearing capacity is continuously increased, and the twisting angle is also continuously increased. When the load reaches about 31 kN, the specimen reaches the ultimate bearing capacity, and finally, the specimen undergoes local buckling failure and flexural-torsional buckling failure. The failure of the specimen is shown in Figure 17.

Figure 17. S-G-Z destroying figure.

The specimen S-Z-Z is a cross-shaped bamboo scrimber column, and there is no obvious change in the early and middle loading periods of the specimen. When the specimen is loaded to about 90 kN, a weak sound of adhesive cracking appears. With the continuous increase of the bearing capacity, the adhesive cracking sound continuously appears. When the loading reaches about 113 kN, the specimen begins to bend integrally, but the bending is not obvious. When the specimen is loaded to about 120 kN, the specimen reaches the ultimate bearing capacity, and finally, the specimen is subjected to instability

failure integrally. After unloading, the specimen basically returns to normal without any damage to the appearance. The failure of the specimen is shown in Figure 18.

Figure 18. S-Z-Z destroying figure.

The specimen S-G-Z-Z is a cross-shaped steel–bamboo scrimber column. There is no obvious phenomenon in the early and middle loading periods of the specimen. When the specimen is loaded to about 93 kN, the sound of adhesive cracking appears. With the continuous increase of the load, the weak sound of adhesive cracking appears occasionally. When the load reaches about 135 kN, the steel plate inside the front flange is severely buckled, and the steel plate inside the rear flange begins to buckle. When the load reaches about 179 kN, the steel plate inside the specimen has wave-type buckling, the gap of the front flange is relatively large, and the other flanges have no obvious buckling effect. When the specimen is loaded to about 181 kN, it reaches the ultimate bearing capacity, and the overall bending phenomenon is obvious. Continue to loading, and the bearing capacity begins to slowly decrease and the test is completed once the bearing capacity drops within the set load range. After unloading, the specimen has a good recovery effect integrally as well as good elastic recovery capacity and toughness, and the ultimate failure of the specimen is instability failure, steel plate buckling, and glue failure. The failure of the specimen is shown in Figure 19.

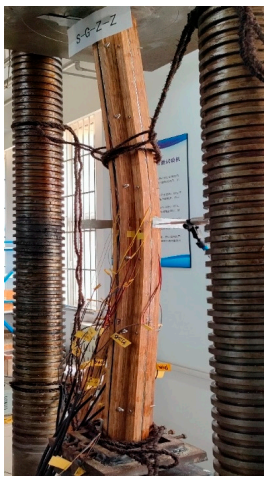

Figure 19. S-G-Z-Z destroying figure.

3.2. Load-Displacement Relationship Curve

It can be seen from Figure 20 and Table 5 that the bearing capacity of the L-shaped steel–bamboo composite special-shaped column is 1.21 times the sum for the L-shaped steel

composite special-shaped column and the L-shaped bamboo composite special-shaped column, which indicates that the bearing capacity of the L-shaped steel–bamboo composite column is increased by 21.36%, and the steel and bamboo scrimber has a good composition effect, which can improve the bearing capacity of the composite specimen. In the early stage of the test, the lateral displacement of the specimen changes little, and the load-displacement curve is basically a linear curve. When the load is increased to about 70% of the ultimate load, the lateral displacement will obviously increase. After reaching the ultimate load, the lateral displacement continues to increase, and the load drops within the set range of the test. At this time, the L-shaped steel composite special-shaped column has obvious buckling, while the L-shaped bamboo and the L-shaped steel–bamboo composite special-shaped column have no obvious failure, and both specimens have instability failure.

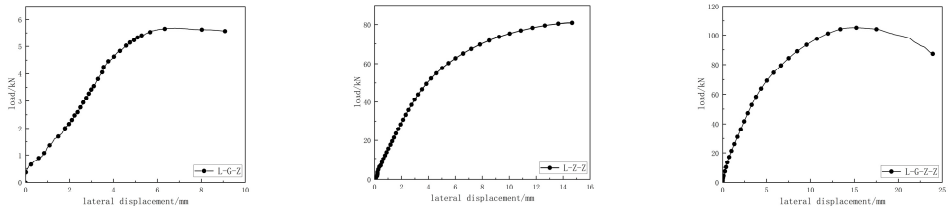

(**a**) (**b**) (**c**)

Figure 20. Load-lateral displacement relationship curve of L-shaped composite special-shaped column. (**a**) L-G-Z load-lateral displacement; (**b**) L-Z-Z load-lateral displacement; (**c**) L-G-Z-Z load-lateral displacement.

Table 5. Test results of L-shaped composite columns.

No.	λ	P_t/kN	Failure Phenomena
L-G-Z	71.8	5.68	Local buckling + flexural-torsional buckling
L-Z-Z	62.1	80.99	Instability failure + glue failure
L-G-Z-Z	38.4	105.18	Instability failure + glue failure + plate buckling

It can be seen from Figure 21 and Table 6 that the bearing capacity of the T-shaped steel–bamboo composite special-shaped column is 19.01% higher than that of the T-shaped steel composite special-shaped column and the T-shaped bamboo composite special-shaped column. In the early loading stage, the specimen is in the linear stage, and the lateral displacement changes little. When the load reaches about 85% of the ultimate load, the lateral displacement begins to increase rapidly, the specimen is bent and deformed integrally, and the lateral displacement in the column is the largest. After the ultimate load is reached, the load will decrease slowly, and the lateral displacement will continue to increase. From Figure 21c, it can be seen that the load-lateral displacement curve of the specimen occasionally fluctuates, which indicates that with the increasing of the load, there is continuous glue failure between the steel and the bamboo scrimber. Finally, the T-shaped steel composite special-shaped column is subjected to flexural-torsional buckling failure, while the T-shaped bamboo and the T-shaped steel–bamboo composite special-shaped columns have instability failure.

It can be seen from Table 7 the bearing capacity of the cross-shaped steel–bamboo composite special-shaped column is 19.52% higher than the sum of that for the cross-shaped steel composite special-shaped column and the cross-shaped bamboo composite special-shaped column. It can be seen from Figure 22a that, due to the flexural-torsional buckling failure of the cross-shaped steel special-shaped column during the test, the load increases irregularly, and the ultimate failure is flexural-torsional failure. It can be seen from Figure 22b that, before the cross-shaped bamboo special-shaped column is loaded to about 20 kN, there is basically no lateral displacement. When the specimen is loaded continuously, it reaches the linear stage, and the load-lateral displacement curve keeps a linear growth

relationship. When the loading is continued to 70% of the ultimate load, the curve slope gradually decreases, the specimen has obvious overall bending, and the ultimate failure is bending instability failure. It can be seen from Figure 22c that the cross-shaped steel–bamboo composite special-shaped column has no obvious lateral displacement before it is loaded to about 30 kN. When the specimen is loaded continuously, the load-lateral displacement develops with a large slope. When the load reaches about 70% of the ultimate load, the lateral displacement gradually and rapidly increases, and finally, the overall bending instability failure occurs.

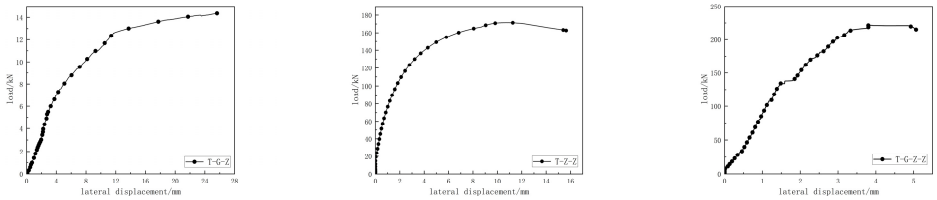

(**a**) (**b**) (**c**)

Figure 21. Load-lateral displacement relationship curve of T-shaped composite special-shaped column. (**a**) T-G-Z load-lateral displacement; (**b**) T-Z-Z load-lateral displacement; (**c**) T-G-Z-Z load-lateral displacement.

Table 6. Test results of T-shaped composite columns.

No.	λ	P_t/kN	Failure Phenomena
T-G-Z	61.3	14.82	Distortional buckling + flexural-torsional buckling
T-Z-Z	46.7	171.51	Instability failure + glue failure
T-G-Z-Z	45.4	221.76	Instability failure + glue failure + plate buckling

Table 7. Test results of cruciform composite special-shaped columns.

No.	λ	P_t/kN	Failure Phenomena
S-G-Z	50.0	31.62	Distortional buckling + flexural-torsional buckling
S-Z-Z	44.4	120.31	Instability failure + glue failure at the end
S-G-Z-Z	43.1	181.58	Instability failure + glue failure + fiber tear

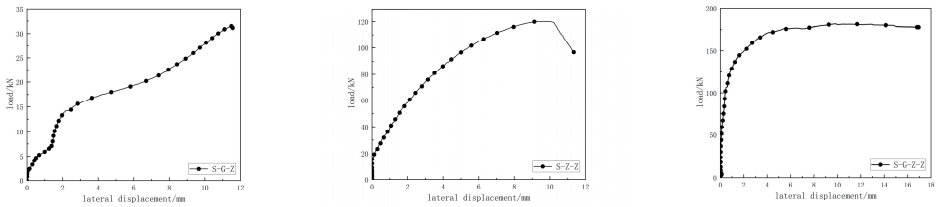

(**a**) (**b**) (**c**)

Figure 22. Load-lateral displacement curve of the cross-shaped composite special-shaped column.(**a**) S-G-Z load-lateral displacement; (**b**) S-Z-Z load-lateral displacement; (**c**) S-G-Z-Z load-lateral displacement.

3.3. Load–Strain Relationship Curve

From the load–strain relationship in Figure 23a, it can be seen that the L-shaped steel special-shaped column is in the elastic stage before being loaded to 50% of the ultimate load, and all strains increase linearly. When the load reaches about 4 kN, the specimen is transformed into the elastic-plastic stage; steel 1 and steel 2 of the strain gauge reach the yield load, the strain increases rapidly compared with the previous stage, and the strain of the specimen continues to increase for a period of time after the load reaches the ultimate load.

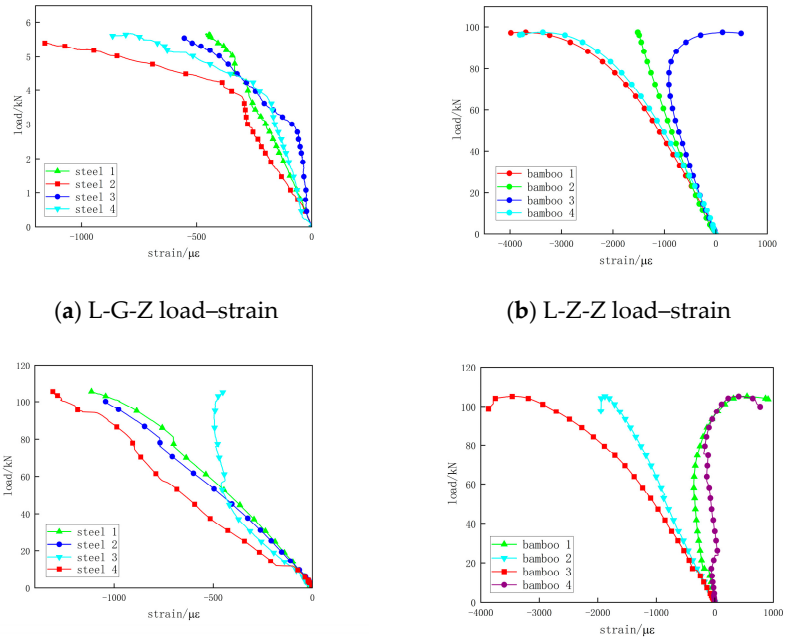

(**a**) L-G-G load–strain (**b**) L-Z-Z load–strain

(**c**) L-G-Z-Z steel load–strain (**d**) L-G-Z-Z bamboo load–strain

Figure 23. Load–strain relationship curve of T-shaped composite special-shaped column.

From the load–strain relationship in Figure 23b, it can be seen that the strain of the bamboo scrimber is larger than that of the steel. At the initial stage of loading, the specimen is in the elastic stage, and the strain increases uniformly with the increase of the load; when the load reaches about 50% of the ultimate load, bamboo 1 and bamboo 2 of the strain gauge are compressed, bamboo 3 is in a linear growth trend, bamboo 4 is in tension, and the specimen begins to bend integrally. When the loading is continued, the slope of load–strain begins to decrease constantly, the strain rapidly increases, and the overall bending deformation occurs. When the specimen reaches the ultimate load, the bearing capacity of the specimen slowly decreases with the increase of the vertical displacement, which indicates that the bamboo scrimber is not subject to brittle failure, and the bamboo scrimber structure has good elastic recovery capability and toughness.

It can be seen from Figure 23c,d that, under the same load, the strain of the bamboo scrimber is greater than that of steel. At the initial stage of loading, the strain curves of steel and bamboo scrimber are in the linear stage; as the load increases to 60% of the ultimate load, they reach the elastic-plastic stage, and difference occurs in the four surfaces. Bamboo 1 and bamboo 4 of the strain gauges are in tension, while bamboo 2 and bamboo 3 of the strain gauges are in compression, and the specimen undergoes bending deformation. After loading to the ultimate load, the strain of the specimen continuously increases. After being loaded in the later stage, the stress of the specimen is borne by the bamboo scrimber. Through comparison, the load-bearing capacity of the steel–bamboo composite column is obviously higher than that of the steel column and the bamboo column, which shows that steel and bamboo collaborate well.

It can be seen from Figure 24a that the T-shaped steel special-shaped column is in the elastic stage before being loaded to about 40% of the ultimate load, the strain of the strain gauge increases linearly with the increase of the load, and the specimen begins to bend and twist. When it is loaded to about 12 kN, the bending and torsion phenomenon of the specimen is intensified; steel 1 of the strain gauge is in tension, and the rest of the steel is in compression.

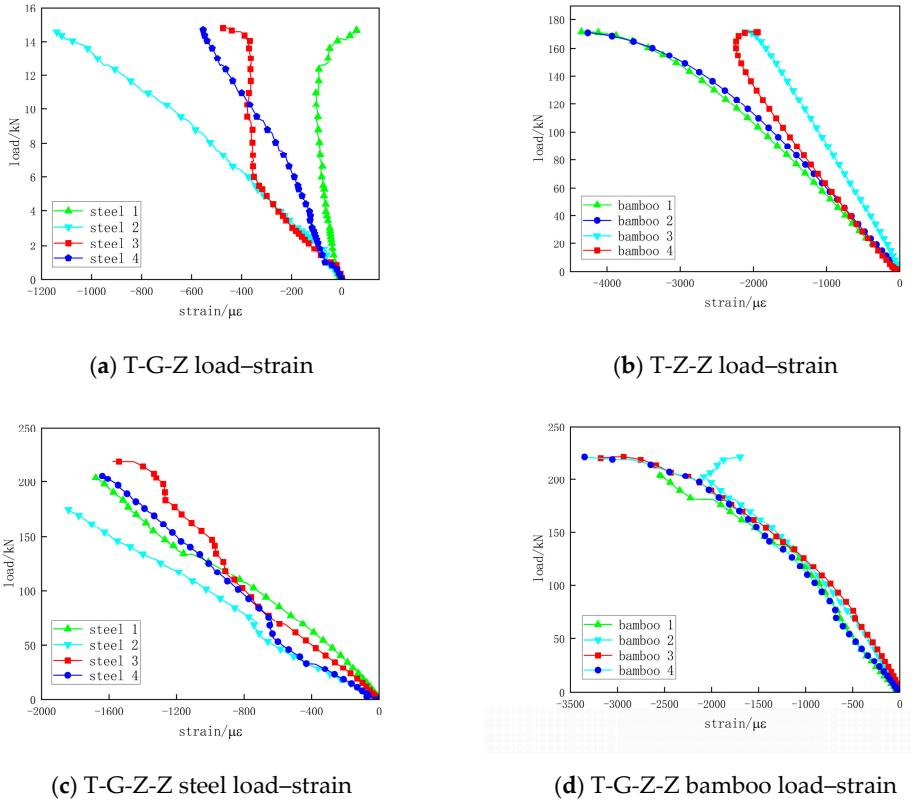

(**a**) T-G-Z load–strain

(**b**) T-Z-Z load–strain

(**c**) T-G-Z-Z steel load–strain

(**d**) T-G-Z-Z bamboo load–strain

Figure 24. Load–strain relationship curve of T-shaped composite special-shaped column.

It can be seen from Figure 24b that the T-shaped bamboo special-shaped column is in the elastic stage before being loaded to about 60% of the ultimate load; all strains increase linearly, and the overall bending effect is not obvious. When the loading is continued, the specimen is transformed into the elastic-plastic stage, the slope of the load–strain curve for bamboo 1 and bamboo 2 begins to decrease slowly, the strain begins to increase rapidly, and the specimen has an obvious bending phenomenon integrally. When the load reaches the ultimate value, all the strain gauges are compressed, and the specimen is subject to overall instability failure.

It can be seen from Figure 24c,d that in the loading process of a T-shaped steel–bamboo composite special-shaped column, steel and bamboo scrimber have the same strain development trend, which is basically maintained in the elastic stage, indicating that steel and bamboo scrimber work together under the action of epoxy resin adhesive and bolt. As the glue failure occurs constantly in the loading process of the test, the load–strain curve of steel shows an uneven growth and all the bamboo load–strain curves are regarded as overlap in the elastic stage, which indicates that the specimen is in the axial compression state.

It can be seen from Figure 25a that the strain value of the specimen is always negative and always under compression. During the loading process, the specimen is basically in the elastic stage, accompanied by flexural-torsional buckling and distortional buckling, and the curve shows an irregular change.

It can be seen from Figure 25b that the cross-shaped bamboo special-shaped column is in the elastic stage until it is loaded to about 70% of the ultimate load. When the loading is continued, the curve slope begins to decrease, presenting two different development trends. The two curves of the same development trend basically coincide, and the specimen has overall bending deformation.

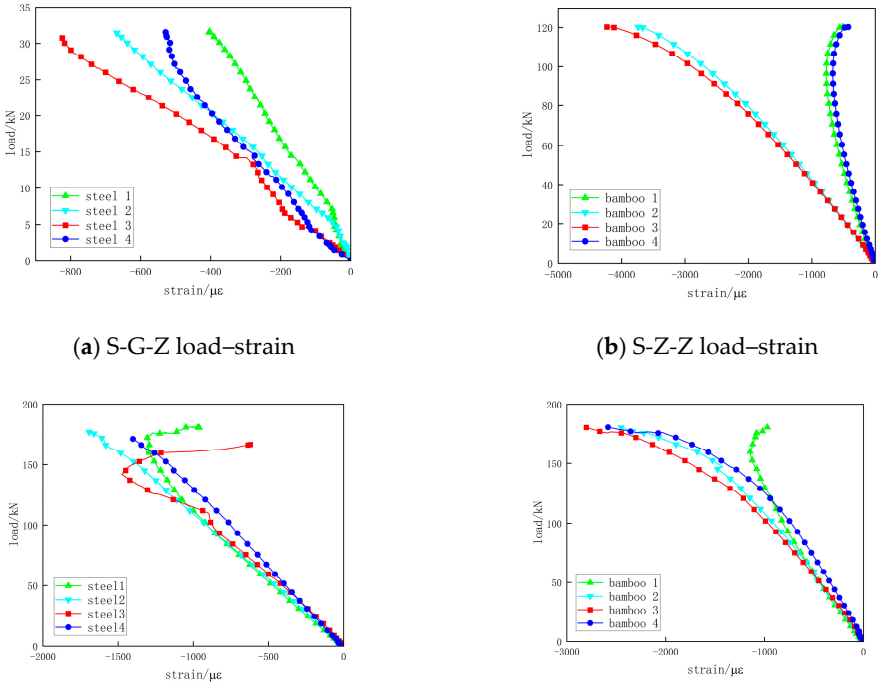

(**a**) S-G-Z load–strain

(**b**) S-Z-Z load–strain

(**c**) S-G-Z-Z steel load–strain

(**d**) S-G-Z-Z bamboo load–strain

Figure 25. Load–strain relationship curve of the cross-shaped composite special-shaped columns.

It can be seen from Figure 25c,d that, at the same stage, the strain of the bamboo scrimber is greater than that of steel. The cross-shaped steel–bamboo composite special-shaped column is in the elastic stage before being loaded to about 50% of the ultimate load, and the strains of all the steels and all the bamboo scrimbers are approximately overlapped, respectively. When the loading is continued, the specimen turns into the elastic-plastic stage, and glue failure constantly occurs in the specimen. During the loading process, the whole specimen is always in the compression state, and all the strain values are negative.

4. Finite Element Analysis

4.1. Establishment of Finite Element Model

The finite element software Abaqus 2021 is used to create finite element models for L-shaped, T-shaped, cross-shaped steel, bamboo, and steel–bamboo special-shaped columns. The components are endowed with material properties according to the specific parameters obtained in the material property test. The material of bamboo scrimber has the natural property of anisotropy [25]. The material of bamboo scrimber has rift grain and cross grain, and the material direction shall be set for it. Set the fiber direction of rift grain as the main direction and that of the cross grain as the secondary direction; the assigned direction of the material is shown in Figure 26. The actual contact surface is a cemented surface, which is set as a surface-to-surface contact type and the slip formula as a small slip; the contact attributes are set as tangential behavior, normal behavior, viscous behavior, and damage. To tightly connect the screw surface with the specimen, set the type as binding.

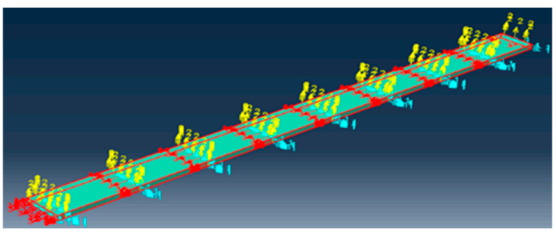

Figure 26. The assignment direction of bamboo scrimber materials.

The first step is to set the elastic buckling analysis and create the analysis step. Select the linear perturbation-buckling analysis as the program type, input 5 for the number of requested characteristic values, set the vector used in each iteration to 10, and the maximum number of iterations at 30. By setting this analysis step, the buckling characteristic value and the corresponding critical load at each stage can be obtained. The second step is to set the non-elastic buckling analysis and create the analysis step. Select the general-static analysis as the program type. In the non-elastic buckling analysis, introduce the initial defect; consider the material and contact of the specimen, and the load value output after the analysis is the load corresponding to the elastic buckling characteristic value.

Set the upper-end constraint of the specimen as translational freedom along the x-axis and y-axis directions and the rotational freedom along the x-axis, y-axis, and z-axis directions. Apply the displacement in the direction z on the reference point of the backing plate and set the lower-end constraint as the translational freedom along the x-axis, y-axis, and z-axis directions and the rotational freedom along the x-axis, y-axis, and z-axis directions. After the setting is completed, conduct the grid division; the model grid division diagram is shown in Figure 27.

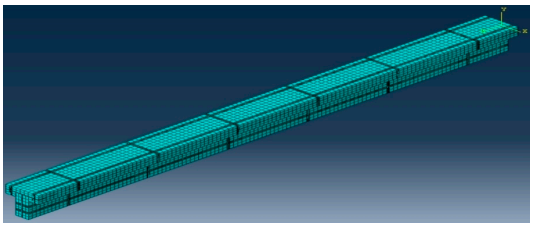

Figure 27. Model grid division diagram.

4.2. Finite Element Results

The stress cloud diagram of the L-shaped column is shown in Figure 28. The middle flange of the L-G-Z specimen is bent, the flange is buckled in a wave shape, and the specimen is bent integrally and has instability failure. The L-Z-Z specimen is bent, the middle part of the long flange is obviously deformed, and the specimen is subject to bending instability failure. The L-G-Z-Z inner steel is buckled in wave shape, and the specimen is obviously bent and has instability failure.

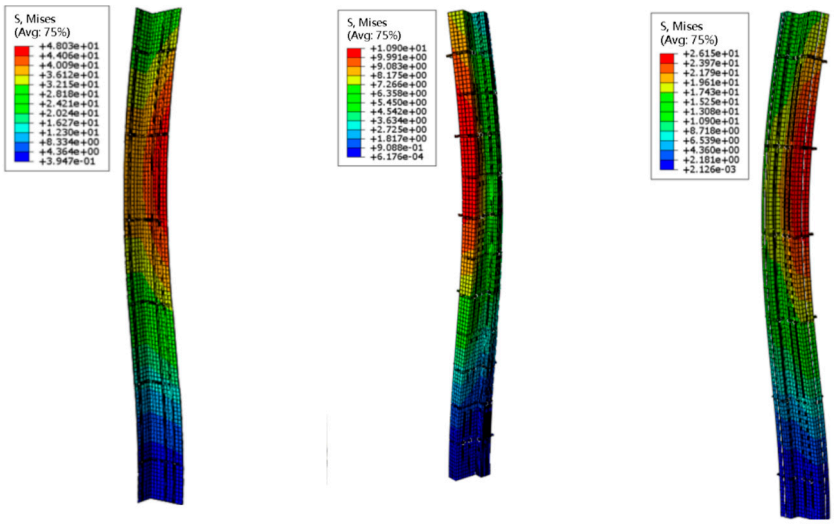

(**a**) L-G-Z cloud diagram (**b**) L-Z-Z cloud diagram (**c**) L-G-Z-Z cloud diagram

Figure 28. Stress cloud diagram of L-shaped column.

Compare the simulated load-axial displacement curve with the test curve, as shown in Figure 29. (1) At the linear stage, the slope of the load-displacement curve in the simulation result is approximately the same as that in the test result, which proves that the rigidity of the finite element model is basically consistent with that of the specimen. (2) For the descending section, the simulation curve and the test curve are relatively flat, which shows that the failure of the specimen is not a brittle failure after reaching the ultimate bearing capacity and has a certain degree of deformation capacity. (3) The simulated ultimate bearing capacity of all the specimens is slightly higher than the ultimate bearing capacity of the test, which indicates that there are some human errors in the components of the test and that the glue failure occurs in the loading process of the test.

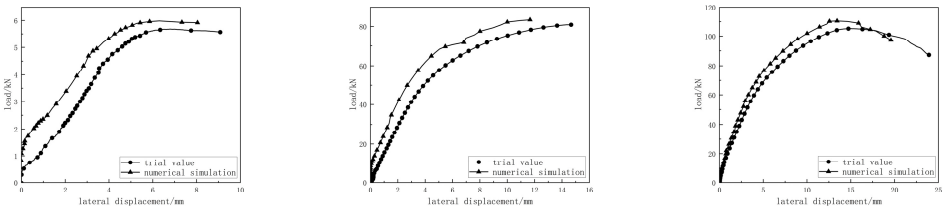

(**a**) (**b**) (**c**)

Figure 29. L-shaped column load-lateral displacement contrast diagram. (**a**) L-G-Z load-lateral displacement; (**b**) L-Z-Z load-lateral displacement; (**c**) L-G-Z-Z load-lateral displacement.

Figure 30 shows the stress cloud diagram of the T-shaped column. The T-G-Z web is bent and twisted towards the flange, and distortional buckling appears in the middle of one flange. The specimen has the failure modes of distortional buckling and flexural-torsional buckling. The T-Z-Z has an obvious bending effect integrally, and the specimen is subject to bending failure integrally. The steel in the middle of T-G-Z-Z has wave-shaped bending, and the specimen is bent integrally; thus, the specimen has instability failure and plate-buckling failure.

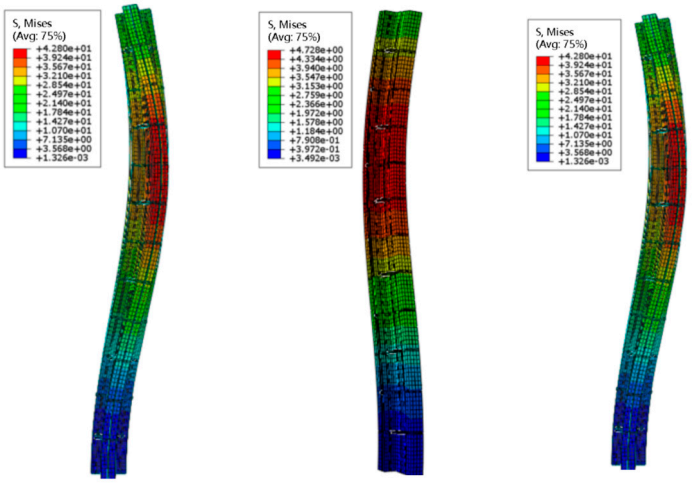

(**a**) T-G-Z cloud diagram(**b**) T-Z-Z cloud diagram(**c**) T-G-Z-Z cloud diagram

Figure 30. T-shaped column stress cloud diagram.

The comparative analysis diagram of the model and the test is shown in Figure 31.

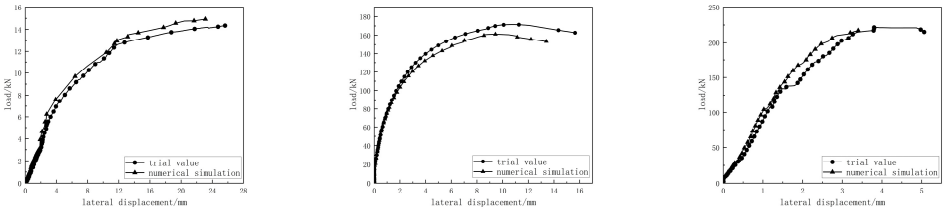

(**a**) (**b**) (**c**)

Figure 31. Load-transverse displacement comparison diagram of T-shaped column. (**a**) T-G-Z load-lateral displacement; (**b**) T-Z-Z load-lateral displacement; (**c**) T-G-Z-Z load-lateral displacement.

(1) The finite element analysis curve and the test curve of all specimens have high similarity, and the general direction is basically the same, which indicates that the finite element model used in this paper can simulate the steel–bamboo composite special-shaped column under the condition of axial compression, verifying that the model has good reliability.

(2) The simulated bearing capacity of all specimens increases faster than that of the test. That is because the elastic modulus and the ultimate bearing capacity of the bamboo scrimber will decrease with the increase of the slenderness ratio in the test process, and the influence of the slenderness ratio is not considered in specific parameters such as the elastic modulus set in the simulation.

Figure 32 shows the stress cloud diagram of the cross-special-shaped column. The front flange of S-G-Z has wave-shaped buckling, it is twisted integrally, and the specimen is subjected to local buckling and flexural-torsional buckling failure. The middle-upper part of S-Z-Z has obvious bending deformation, and finally, the specimen has instability failure. All the internal plates of S-G-Z-Z show wave-shaped buckling; they have obvious bending integrally, and the ultimate failure of the specimen is instability failure and plate buckling.

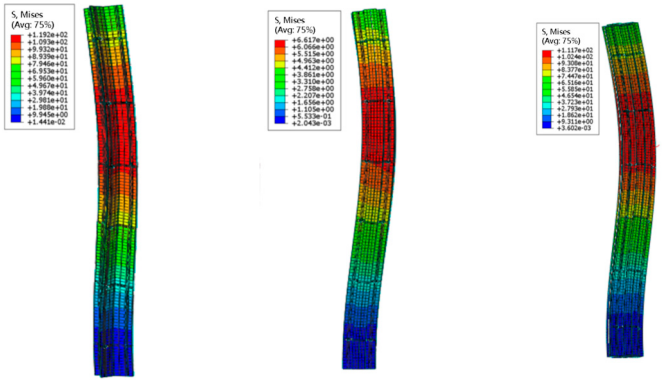

(**a**) S-G-Z cloud diagram(**b**) S-Z-Z cloud diagram(**c**) S-G-Z-Z cloud diagram

Figure 32. Stress cloud diagram of the cross-shaped column.

Compare the simulated load-axial displacement curve with the test curve, as shown in Figure 33. It can be seen that the simulated ultimate bearing capacity of all specimens is slightly higher than the tested ultimate bearing capacity. Due to the problem of the manufacturing process of the specimen, the compressive strength of the specimen cannot be fully developed, but the finite element model can simulate the full compressive strength of the specimen in ideal conditions.

From Table 8, it can be seen that the ultimate bearing capacity of L-G-Z-Z is the sum of L-G-Z and L-Z-Z increased by 23.11%, the ultimate bearing capacity of T-G-Z-Z is the sum of T-G-Z and T-Z-Z increased by 23.43%, and the ultimate bearing capacity of S-G-Z-Z is the sum of S-G-Z and S-Z-Z increased by 14.83%, which indicates that the steel and the bamboo scrimber have a good composition effect, and the bearing capacity of composite specimens can be improved.

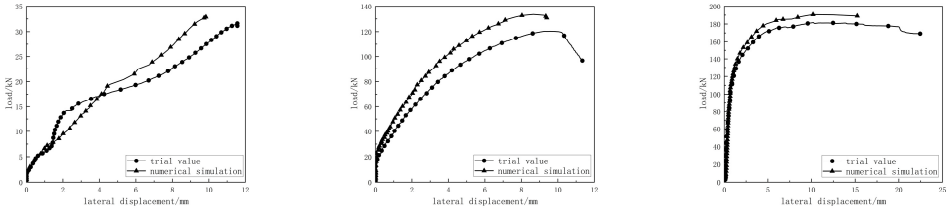

(**a**) (**b**) (**c**)

Figure 33. Comparison of load-transverse displacement of cross-shaped columns. (**a**) S-G-Z load-lateral displacement; (**b**) S-Z-Z load-lateral displacement; (**c**) S-G-Z-Z load-lateral displacement.

Table 8. Comparison of simulation results with experimental results.

Specimen No.	P_A/kN	P_t/kN	P_A/P_t
L-G-Z	6.38 kN	5.68 kN	1.12
T-G-Z	15.34 kN	14.82 kN	1.04
S-G-Z	32.88 kN	31.62 kN	1.04
L-Z-Z	83.73 kN	80.99 kN	1.03
T-Z-Z	160.79 kN	171.51 kN	0.94
S-Z-Z	133.32 kN	120.31 kN	1.11
L-G-Z-Z	110.94 kN	105.18 kN	1.05
T-G-Z-Z	217.39 kN	221.76 kN	0.98
S-G-Z-Z	190.85 kN	181.58 kN	1.05

The maximum value for the ratio of the simulated ultimate bearing capacity to the tested ultimate bearing capacity is 1.12, and the minimum value is 0.94. As there are many factors affecting the actual composite columns, the simulation is in an ideal state, which results in the ultimate bearing capacity of the test being slightly lower than that of the simulation. However, the ratio of the two is very close to 1, which indicates that the simulation results fit well with the test results. The established Abaqus finite element model can simulate well the buckling behaviors of the L-shaped, the T-shaped, and the cross-shaped cold-formed thin-walled steel–bamboo scrimber composite special-shaped columns under axial compression, which has practical significance for engineering applications.

5. Calculations of Bearing Capacity Under Axial Compression

5.1. Basic Assumptions and Calculation Formula

The load–strain is analyzed for three kinds of steel–bamboo composite special-shaped columns as above. From the curve, it can be seen that the strain development trend of cold-formed thin-walled steel and bamboo scrimber is the same during the loading process and is basically maintained in the elastic stage, which indicates that the cold-formed thin-walled steel and the bamboo scrimber work together under the action of epoxy resin adhesive and bolts. When the specimen reaches the ultimate load, the steel reaches the yield state, and the bamboo scrimber material is still in the linear elastic stage without obvious damage. Based on this conclusion, the following three basic assumptions are taken as the basis for deriving the formula:

(1) The cold-formed thin-walled steel–bamboo scrimber composite special-shaped column is suitable for the assumption of a flat section.

(2) When the cold-formed thin-walled steel in the composite special-shaped column reaches the yield state, the specimen reaches the yield state integrally.

(3) Before the specimen reaches the yield state integrally, the cold-formed thin-walled steel and the bamboo scrimber work together in the elastic stage, and they have the same strain change trend.

On the basis of the above-mentioned basic assumptions, the calculation formula for the axial compression capacity of the cold-formed thin-walled steel–bamboo scrimber special-shaped column is derived.

$$N_{cr} = a\varphi\left(f_y A_s + f_b A_b\right) = a\varphi(f_y A_s + \frac{E_b}{E_s} f_y A_b) \quad (5)$$

wherein *Ncr* is the bearing capacity of the composite special-shaped column, kN; a is the equation modification coefficient, φ is the overall stability coefficient of the composite special-shaped column, f_y is the yield strength of cold-formed thin-walled steel, f_b is the compressive strength of bamboo scrimber, A_s is the sectional area of cold-formed thin-walled steel, A_b is the sectional area of the bamboo scrimber, E_s is the elastic modulus of the cold-formed thin-walled steel, and E_b is the elastic modulus of the bamboo scrimber.

5.2. Comparison Between Calculation Results and Experimental Results

From Table 9, it can be seen that the error in the ultimate bearing capacity and experimental value of the composite special-shaped column calculated theoretically is within 13.28%. It is considered that the theoretical calculation formulas of the three composite special-shaped columns can be used for reference in practical engineering. The ultimate bearing capacity of the steel–bamboo composite special-shaped column is obviously higher than the sum of the steel composite special-shaped column and the bamboo composite special-shaped column.

Table 9. Comparison of theoretical formula results and experimental results of bearing capacity.

Specimen No.	Theoretical Value for Calculations in Formula/kN	Experimental Value/kN	Error
L-G-Z	6.43 kN	5.68 kN	13.13%
T-G-Z	12.85 kN	14.82 kN	−13.28%
S-G-Z	34.42 kN	31.62 kN	8.84%
L-Z-Z	81.04 kN	80.99 kN	0.06%
T-Z-Z	151.22 kN	171.51 kN	−11.82%
S-Z-Z	135.88 kN	120.31 kN	12.94%
L-G-Z-Z	110.65 kN	105.18 kN	5.20%
T-G-Z-Z	202.95 kN	221.76 kN	−8.48%
S-G-Z-Z	182.55 kN	181.58 kN	0.53%

6. Conclusions

(1) According to the test, the failures of the steel composite special-shaped column include local buckling, flexural-torsional buckling, and distortional buckling; the failures of the bamboo scrimber special-shaped column include instability failure and glue failure; and the failures of the steel–bamboo scrimber include instability failure, glue failure, and steel-plate buckling failure. After the experiment was completed, the bamboo scrimber composite column and the steel–bamboo composite column basically recovered without any external damage, which indicates that the bamboo scrimber material has good elastic recovery capability and toughness.

(2) The bearing capacity of the L-shaped steel–bamboo composite special-shaped column is 21.4% higher than the sum of the L-shaped steel composite special-shaped column and the L-shaped bamboo composite special-shaped column. The bearing capacity of the T-shaped steel–bamboo composite special-shaped column is 18.8% higher than the sum of the T-shaped steel composite special-shaped column and the T-shaped bamboo composite special-shaped column. The bearing capacity of the cross-shaped steel–bamboo composite special-shaped column is 19.5% higher than the sum of the cross-shaped steel composite special-shaped column and the cross-shaped bamboo composite special-shaped column.

(3) The calculation formula for the axial compression bearing capacity of the three kinds of composite special-shaped columns is derived. Compared with the experimental

data, the error in the theoretical value and the experimental value of the ultimate bearing capacity of the composite special-shaped columns is within 13.28%, which proves that the theoretical formula has a certain reliability for calculating the ultimate bearing capacity of the composite special-shaped columns.

(4) In the simulating condition, the composite special-shaped column is in the ideal state, so the simulated ultimate bearing capacity is generally higher than the ultimate bearing capacity in the experiment, but the ratio of both is 0.94–1.12. Meanwhile, the failure process of the specimen is almost the same under the experimental study and the simulation analysis, and the simulation results fit well with the experimental results, which indicate that the finite element model is suitable for simulating the composite special-shaped column.

(5) According to the experimental research, theoretical analysis, and numerical simulation comparison analysis, it can be known that steel and bamboo scrimber work together and have a good composition effect; the steel–bamboo composite special-shaped column has obviously higher ultimate bearing capacity and increased deformation capacity, and the bearing capacity of L-shaped section is improved most obviously.

Author Contributions: Conceptualization, C.L., Y.W. and B.Y.; methodology, J.H. and X.F.; software, Y.W.; validation, C.L. and B.Y.; formal analysis, Y.W. and C.L.; investigation, C.L.; resources, J.H. and B.Y.; data curation, C.L. and Y.W.; writing—original draft preparation, C.L., B.W. and B.Y.; writing—review and editing, Y.W. and C.L.; visualization, C.L. and Y.W.; supervision, J.H., B.W. and X.F.; project administration, J.H.; funding acquisition, J.H. All authors have read and agreed to the published version of the manuscript.

Funding: This research was funded by the National Natural Science Foundation of China (51678237) and (51208171).

Data Availability Statement: The original contributions presented in the study are included in the article, further inquiries can be directed to the corresponding author.

Conflicts of Interest: The authors declare no conflict of interest.

References

1. Yu, R.; Spiesz, P.; Brouwers, H.J.H. Effect of nano-silica on the hydration and microstructure development of Ultra-High Performance Concrete (UHPC) with a low binder amount. *Constr. Build. Mater.* **2014**, *65*, 140–150. [CrossRef]
2. Li, X. Study on Bearing Capacity of Bolted Joints of Bamboo Scrimber. Ph.D. Thesis, China Academy of Forestry Sciences, Beijing, China, 2013.
3. Zhang, Q. *Industrial Utilization of Bamboo in China*; China Forestry Publishing House: Beijing, China, 1995.
4. Song, X.; Liu, X. Industrialized Utilization of Bamboo. *For. Sci. Technol.* **2011**, *36*, 55–57.
5. Huang, Z.; Li, C.; Wu, Y. Application of bamboo in civil engineering. *For. Eng.* **2007**, *22*, 79–80.
6. Yan, S.; Li, Y. Analysis of Application Prospect of Bamboo in Building Structure. *For. Eng.* **2008**, *24*, 62–65.
7. Wu, Y.; Li, Y.; Ge, B. Application and Prospect of Modified Bamboo. *For. Eng.* **2008**, *24*, 68–71.
8. Yall, W.M.; Xie, Z.Q.; Song, L.L.; He, H.-X. Study on the mechallical propeny of self-piercing rivet and its constinltive model in cold-fomed thin-walled steel. *Eng. Mech.* **2017**, *34*, 133–143.
9. Yao, X. Design reliability analysis of cold-formed thin-walled steel members with lipped channel sections considering distortional buclding. *Open Civ. Eng. J.* **2017**, *11*, 906–918.
10. Wu, M. Study on the Axial Compression Performance of Built-in Steel Reinforced Bamboo Scrimber. Master's Thesis, Northeast Forestry University, Harbin, China, 2022.
11. Ge, Y.; Li, Y.; Tong, K.; Zhang, J. Study on shear performance of thin-walled steel-recombined bamboo composite I-beam. *For. Eng.* **2018**, *34*, 72–79.
12. Zhang, X.; Zeng, Z. Finite element analysis of cold-formed thin-walled steel-recombined bamboo composite columns under eccentric compression. *Shanxi Constr.* **2018**, *44*, 45–46.
13. Mao, M.; Zhang, J.; Tong, K.; Li, Y. Comparative analysis of bending performance of steel-bamboo composite beams based on different kinds of bamboo plates. *Build. Struct.* **2020**, *50*, 107–113.
14. Mahdavi, M.; Cloustion, P.L.; Arw Ade, S.R. Development of laminated bamboo lunber: Review of processing, performance, and economical considerations. *J. Mater. Cival Eng.* **2011**, *23*, 1036–1042. [CrossRef]
15. Hebel, D.E.; Javadian, A.; Helsel, F.; Schlesier, K.; Griebel, D.; Wielopolski, M. Processing-controlled optimization of the tensile srenth of bamboo fiber composites for structural applications. *Compos. Part B Eng.* **2014**, *67*, 125–131. [CrossRef]

16. Zakikhani, P.; Zahari, R.; Sultan, M.T.H.; Majid, D.L. Extraction and preparation of bamboo fiber-reinforced composites. *Materals Des.* **2014**, *63*, 820–828.
17. van der Lugt, P.; van den Dobbelsteen, A.A.J.F.; Janssen, J.J.A. An environmental, economic and practical assessment of bamboo as a building material for supporting structures. *Constr. Build. Mater.* **2006**, *20*, 648–656. [CrossRef]
18. Yu, D.W.; Tan, H.W.; Ruan, Y.G. A future bamboo-structure residential building prototype in China: Life cycle asscssment of energy use and carbon emission. *Energy Build.* **2011**, *43*, 2638–2646. [CrossRef]
19. Liu, S.M.; Liu, J.S. New building material-the development and application of recombinant bamboo. *Adv. Mater. Res.* **2013**, *773*, 441–444. [CrossRef]
20. Hang, W.; Fu, W.; Zhou, J.; Zhang, Z.; Chen, Z. A preliminary study on bamboo original state multi recombination building material. *Wood Process. Mach.* **2014**, *25*, 20+39–41.
21. *GB/T50329-2012*; Standard for Test Methods of Timber Structures. China Construction Industry Press: Beijing, China, 2002.
22. *GB/T40247-2021*; Bamboo Scrimber. China Standards Publishing House: Beijing, China, 2021.
23. *GB/T1938-2009*; Test Method for Tensile Strength Parallel to Grain of Wood. China Standard Publishing House: Beijing, China, 2009.
24. *GB50018-2002*; Technical Code for Cold-Formed Thin-Walled Steel Structures. China Planning Press: Beijing, China, 2002.
25. Zhang, X.; Jing, E.; Li, Y.; Zhang, Y. Experimental study on compressive and flexural mechanical properties of reconstituted bamboo. *Ind. Build.* **2016**, *46*, 7–12.